Advances in Energy and Materials Research https://jaem.qom.ac.ir/

Hydrogen storage capacity of NH_2M^+ (M=Be, Li, Sc, Ti, V, and Ca) compounds: DFT and molecular dynamics outlook

Rezvan Rahimi✉1, **Mohammad Solimannejad**✉2 **and Ajay Chaudhari**3

1. Correspinding authoer, Department of Chemistry, Faculty of Science, University of Arak, Arak, Iran. Email: r-rahimi@araku.ac.ir
2. Correspinding authoer, Department of Chemistry, Faculty of Science, University of Arak, Arak, Iran. Email: m-solimannejad@araku.ac.ir
3. Department of Physics, the Institute of Science, Dr. Homi Bhabha State University, Mumbai, India.

Article Info	ABSTRACT
Article type: Research Article **Article history:** Received 22 May 2024 Received in revised form 27 Jul 2024 Accepted 28 Sep 2024 Published online 25 Dec 2024 **Keywords**: Hydrogen storage; DFT and MP2; Molecular dynamics.	This study evaluates the hydrogen storage capabilities of NH2M+ compounds (where M = Be, Li, Sc, Ti, V, Ca) using density functional theory (DFT) and second-order Møller-Plesset (MP2) methods with the 6-31++G(d,p) basis set. Our findings demonstrate that NH2Be+, NH2Li+, NH2Sc+, NH2Ti+, NH2V+, and NH2Ca+ complexes can bind up to three, five, six, six, five, and eight H2 molecules, respectively, achieving gravimetric hydrogen uptake capacities of 19.3%, 30.3%, 16.4%, 15.8%, 12.9%, and 22.2%. These capacities significantly surpass the U.S. Department of Energy's 2025 target of 5.5 wt%. Gibbs free energy-corrected adsorption energy analyses indicate that H2 adsorption on NH2Be+, NH2Ti+, and NH2V+ complexes is thermodynamically favorable at room temperature across a broad pressure and temperature range (50–400 K, 50–400 atm). In contrast, adsorption on NH2Li+, NH2Sc+, and NH2Ca+ complexes is viable below 85 K, 135 K, and 75 K, respectively. High desorption temperatures for NH2Be+, NH2Sc+, NH2Ti+, and NH2V+ complexes reflect their robust interactions with H2 molecules compared to other NH2M+ variants. Molecular dynamics simulations using atom-centered density matrix propagation (ADMP) at ambient conditions reveal that some adsorbed H2 molecules dissociate from the complexes. Overall, NH2Ti+ emerges as a particularly promising candidate for efficient hydrogen storage due to its favorable adsorption characteristics and high capacity.

Cite this article: Rahimi, R. & et al, (2024). Hydrogen storage capacity of NH^2M^+ (m=be, li, sc, ti, v, and ca) compounds: dft and molecular dynamics outlook, *Advances in Energy and Materials Research, 1* (4), 1-10. https://doi.org/10.22091/jaem.2025.13007.1025

DOI: 10.22091/jaem.2025.13007.1025

Publisher: University of Qom.

1. Introduction

Hydrogen is the third most abundant element on the Earth's surface. Its potential as a fuel for hydrogen storage has garnered significant attention from researchers in recent years, owing to its unique properties as a renewable energy carrier, its safety, and its suitability as an ideal fuel. Despite the challenges associated with hydrogen production and the need for larger storage volumes, it has the potential to replace fossil fuels, which are known to contribute to air pollution and damage the ozone layer. Realizing a hydrogen economy [1] and utilizing hydrogen as a fuel in the future [2, 3] is not a straightforward endeavor; it necessitates overcoming the challenges associated with hydrogen storage. Recently, solid-state hydrogen storage has been proposed as a solution to the inefficiencies of hydrogen storage in automotive fuel cells [4]. If storage systems for hydrogen can be improved, hydrogen could become a viable fuel for the automotive sector. The properties of an effective hydrogen storage system should include affordability, safety, and ease of transportation. Furthermore, such a system should meet the technical requirements set forth by the U.S. Department of Energy (DOE) by 2025 [5]. One of the most effective methods for storing hydrogen is through adsorption on solid-state materials in molecular form. For these materials to be suitable for vehicular applications, hydrogen storage must be energetically favorable at room temperature and 1 atm pressure. Therefore, it is imperative to identify an ideal material to ensure that the hydrogen economy does not remain a hypothetical concept.

Various materials have been explored for hydrogen storage, including metal hydrides [6-10], chemical hydrides [11], small organometallic complexes [12-15], and inorganometallic complexes [16-19]. Research groups have investigated Be/Sc-doped pentalene (C_8H_6), alkali and alkaline earth metal-doped B_6H_6, among others, for hydrogen storage [20-23]. They predicted that the H_2 uptake capacities of the C_2H_4Be and $C_2H_4Be_2$ complexes, which can adsorb two and four H_2 molecules, are 10.3 and 15.5 wt% H_2, respectively [24]. Recent studies have shown that Sc-doped small organometallic complexes exhibit higher H_2 uptake capacities [25-27]. Wadnerkar et al. observed that the H_2 uptake capacity of the C_2H_4Sc cation is greater than that of its neutral and anionic forms [28]. Notably, the H_2 storage capacities of C_2H_4V and its cation are predicted to be 11.32 and 13.28 wt%, respectively [29], while C_2H_4Ti and its cation differ by about 2 wt% [30]. Additionally, Ti-doped acetylene shows a stronger interaction with H_2 molecules compared to Na, K, and Li-doped acetylene [15].

The hydrogen uptake capacity of magnesium and lithium-doped boranes has been investigated using Møller-Plesset perturbation theory and density functional theory (DFT) by Pathak et al. [31]. The interaction energy per H_2 molecule ranges from 5.47 to 15.67 kcal/mol, making it suitable for hydrogen storage under ambient conditions. Most studies referenced focus on the hydrogen storage capacity of metal-decorated inorganic complexes.

In recent years, alkali metal amines have played a significant role in advancing the field of chemistry [32-35]. In the 1950s [36], three-dimensional structures of solid alkali metal amines were examined using infrared (IR) spectroscopy [37] and nuclear magnetic resonance (NMR) spectroscopy. One of the earliest attempts to synthesize lithium amine occurred at the end of the last century through the reactive milling of Li_3N at 20 bar hydrogen pressure for 4 hours [38]. This structure represents the simplest lithium amine utilized in synthesis and structural studies. Furthermore, the structural properties and electron transfer reactivity of NX_3/NX_3^+ (where X=H, F) systems have been theoretically investigated [39]. Notably, the NH_3/NH_3^+ system has garnered considerable attention from researchers due to its prevalence in nature and biological chemistry, and it has been explored through both experimental [40,41] and theoretical [42,43] methods.

In 2004, Sun et al. [44] determined the electron transfer reactivity of methyl-substituted amines, specifically the neutral molecules [NH_3, NH_2CH_3, $NH(CH_3)_2$, and $N(CH_3)_3$] and their corresponding cations [NH_3^+, $NH_2CH_3^+$, $NH(CH_3)_2^+$, and $N(CH_3)_3^+$]. Consequently, it would be worthwhile to investigate the NH_3/NH_3^+ system, focusing on the effects of substituting one hydrogen atom with alkali metals, alkaline earth metals, and transition metals on reactivity.

In this study, we examined the hydrogen storage capacity of NH_2M^+ compounds, where M represents Be, Li, Sc, Ti, V, and Ca, utilizing DFT and second-order Møller-Plesset (MP2) calculations. We focused on NH_2M^+ cations doped with alkali metals, alkaline earth metals, and transition metals, to evaluate their potential to meet the targets set by the U.S. Department of Energy (DOE) for vehicular applications under ambient conditions.

The selection of NH_2M^+ compounds is based on several key factors: First, the hydrogen uptake capacity of all studied complexes exceeds the target set by the US Department of Energy (5.5 wt% by 2025). Secondly, our desired complex, which exhibits high desorption temperatures, demonstrates a stronger interaction with H_2 molecules compared to previously studied complexes conducted by other researchers. Additionally, we have examined the variations in structural parameters before and after hydrogen adsorption, including the averaged adsorption energy without (ΔE) and with zero point (ΔE_{ZPE}), Gibbs free energy corrected adsorption energies (ΔE_G), hydrogen uptake capacity (W%), desorption temperature (TD), the temperature/pressure dependence of adsorption energies for the NH_2M^+ complexes (M = Be, Li, Sc, Ti, V, and Ca), and molecular dynamics (MD) simulations.

2. Computational Details

Geometry optimizations were conducted using the MP2 method [45] and DFT with the wB97XD functional [46], utilizing a 6-31++G(d,p) basis set. No symmetry constraints have been imposed on the complexes during optimization, which has been performed using the Gaussian09 software [47]. Molecular electrostatic potential (MEP) and partial density of states (PDOS) analyses for all $NH_2M^+(nH_2)$ complexes were executed at the MP2/6-31++G (d, p) level, with PDOS plots generated using the Gauss Sum program [48]. Charge transfer between the H_2 molecule and the NH_2M^+ has been evaluated through natural bond orbital (NBO) analysis [49]. In this study, the HOMO–LUMO gap (HLG) is determined using Equation (1), where ε_H and ε_L denote the energies of the highest occupied molecular orbital (HOMO) and the lowest unoccupied molecular orbital (LUMO), respectively.

$$HLG = \varepsilon_L - \varepsilon_H \tag{1}$$

The averaged adsorption energies, both without zero-point energy correction (ΔE) and with zero-point energy correction (ΔE_{ZPE}), as well as the Gibbs free energy correction (ΔE_G), for all complexes have been obtained using Equations (2-4).

$$\Delta E = \{E[NH2M+] + (n \times E[H_2]) - E[NH_2M^+(nH_2)]\}/n \tag{2}$$

$$\Delta E_{ZPE} = \{E_{ZPE}[NH_2M^+] + (n \times E_{ZPE}[H_2]) - E_{ZPE}[NH_2M^+(nH_2)]\}/n \tag{3}$$

$$\Delta E_G = \{E_G[NH_2M^+] + (n \times E_G[H_2]) - E_G[NH_2M^+(nH_2)]\}/n \tag{4}$$

In this work, the H_2 desorption temperature (TD) has been obtained using the van't Hoff equation [50]:

$$TD = (\Delta E_{ZPE}/k_B)\,((\Delta S/R) - LnP)^{-1} \tag{5}$$

Where k_B is the Boltzmann constant (1.38×10^{-23} JK^{-1}), R is the gas constant (8.31 $JK^{-1}Mol^{-1}$), ΔS the change in the H_2 entropy from gas to liquid phase [51], and P is the equilibrium pressure P (1 atm). The molecular dynamics (MD) simulations have been performed using atom-centered density matrix propagation (ADMP) at 300 K and 1 atm pressure. The time step (Δt) of ADMP-MD was set at 0.2 fs. The temperature has been maintained using the velocity scaling method during the ADMP-MD simulations.

3. Results and Discussion

The NH_3 and NH_3^+ systems exhibit C_{3V} and D_{3h} symmetry, respectively, with two degenerate asymmetric stretching frequencies of 3607.8 cm^{-1} and 3515.2 cm^{-1}. Additionally, the NH_3^+ system consists of two pairs of degenerate vibrational frequencies (ω2, ω3 and ω5, ω6). Previous studies have indicated that the NH_3^+ system, with an ∠HNH bond angle of 120.2º, is theoretically predicted to have a planar structure [39]. Consequently, NH_2M^+ compounds have formed by substituting one hydrogen atom in the NH_3^+ molecule with alkali metals, alkaline earth metals, and transition metals. Given that NH_2M^+ compounds are obtained by replacing one hydrogen atom with the desired substituents, the objective of this study is to investigate the hydrogen storage capacity of NH_2M^+ compounds.

The optimization of the NH_2M^+ compounds (where M = Be, Li, Sc, Ti, V, and Ca) (refer to Fig. 1) and the corresponding NH_2M^+ (nH_2) complexes (see Fig. 2) was conducted using the MP2 and DFT with the wB97XD functional, employing the 6-31++G (d, p) basis set.

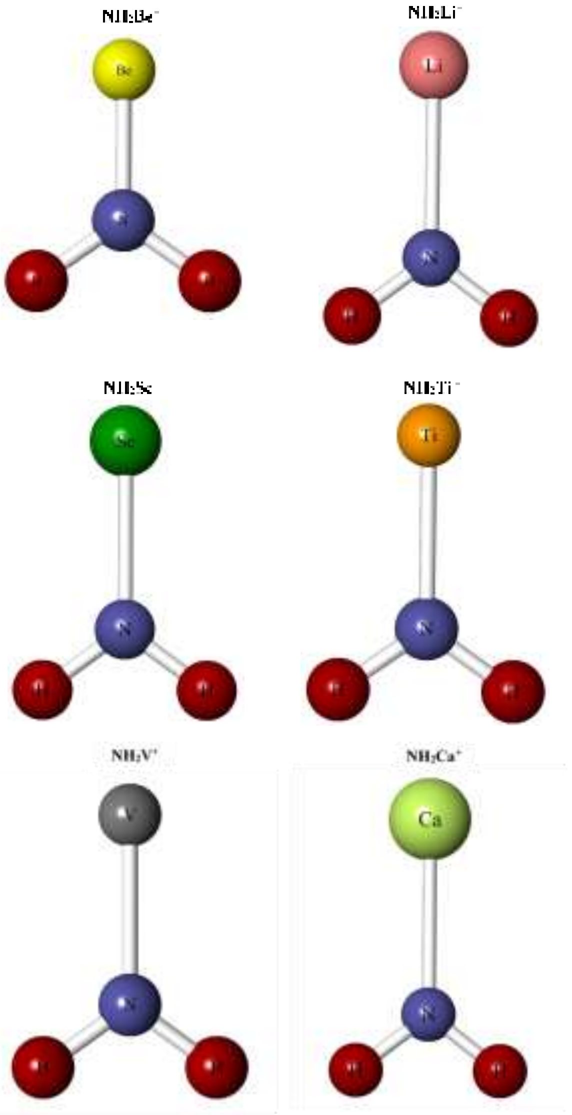

Fig.1. Optimized geometries of pristine NH2M+ compound, where M is Be, Li, Sc, Ti, V, and Ca.

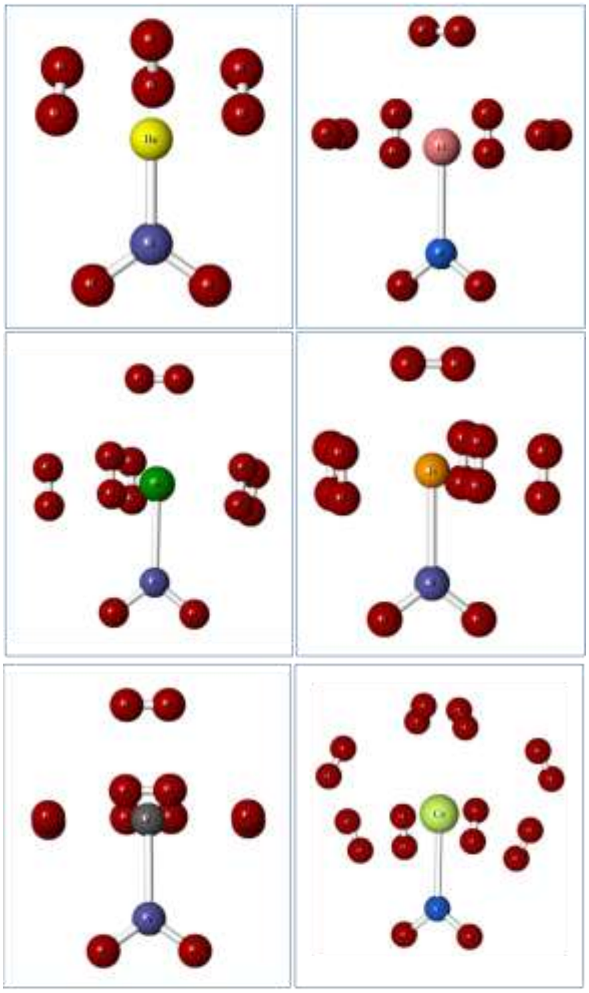

Fig. 2. Optimized geometries stable configurations of NH2M+(nH2) complex, where M is Be, Li, Sc, Ti, V, and Ca.

The natural bond orbital (NBO) analysis for all considered complexes, both before and after H_2 adsorption, was conducted at the MP2/6-31++G (d, p) level and is presented in Table 1. The results in Table 1 indicate that in all complexes, the charge on the metal atom (M = Be, Li, Sc, Ti, V, and Ca) becomes negative due to charge acceptance. According to Table 1, the total charge on the adsorbed H_2 molecules follows this order: $NH_2V^+ > NH_2Ti^+ > NH_2Be^+ > NH_2Sc^+ > NH_2Ca^+ > NH_2Li^+$, with values ranging from 0.042 to 1.304 e. In the NH_2Be^+, NH_2Li^+, NH_2Sc^+, NH_2Ti^+, NH_2V^+, and NH_2Ca^+ compounds, the M atoms become less negative after H_2 adsorption, exhibiting charges of -0.539, -0.040, -0.481, -1.524, -1.269, and -0.284, respectively.

Table1. NBO charges for $NH_2M^+(nH_2)$ complexes before and after H_2 adsorption at MP2/6-311++g(d,p) level (The values in parenthesis are NBO charges before H_2 adsorption, where M is Be, Li, Sc, Ti, V, and Ca).

System		N	H	M	H_2
$NH_2M^+(nH_2)$	$NH_2Be^+(3H_2)$	-0.925 (-0.758)	0.320 (0.345)	0.529 (1.068)	0.759
	$NH_2Li^+(5H_2)$	-0.435 (-0.439)	0.327 (0.330)	0.739 (0.779)	0.042
	$NH_2Sc^+(6H_2)$	-1.281 (-1.042)	0.394 (0.323)	0.914 (1.395)	0.580
	$NH_2Ti^+(6H_2)$	-0.947 (-1.177)	0.392 (0.353)	-0.053 (1.471)	1.215
	$NH_2V^+(5H_2)$	-0.746 (-0.569)	0.416 (0.344)	-0.389 (0.880)	1.304
	$NH_2Ca^+(8H_2)$	-1.184 (-1.236)	0.321 (0.301)	1.351 (1.635)	0.192

To enhance the accuracy of display and improve the understanding of why H_2 molecules are adsorbed on M atoms of NH_2M^+ compounds, we present the calculated maps of electrostatic potential (MEP) (see Fig. 3) and the partial density of states (PDOS) plots for the considered complexes (see Fig. 4). The MEP analysis for NH_2M^+ compounds reveals that these desired compounds can induce polarization to the adsorbed H_2 molecules by induce the electrostatic field. Consequently, a significant factor contributing to the adsorption of H_2 on NH_2M^+ complexes is the enhanced ability of the H_2 molecule to adsorb under electrostatic interactions. As illustrated in Fig. 3, the highest electron density is localized around the M atom in all NH_2M^+ complexes, indicating that the M atom serves as the most favorable adsorption site for H_2 molecules.

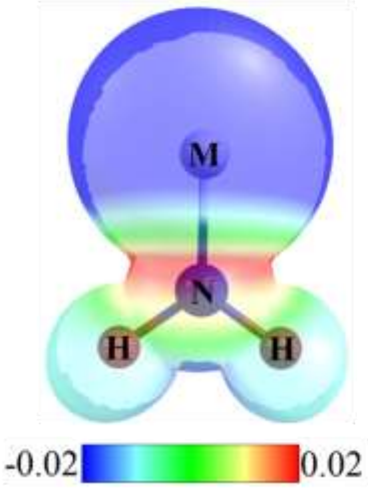

Fig. 3. The presentation MEP surface of the NH2M+ compound, the surfaces are specified by the 0.0004 electrons/b3 contour of an electronic density and color ranges in a.u.

The analysis of the PDOS spectra clearly indicates the percentage contribution of the orbitals of H_2 molecules adsorbed on NH_2M^+ complexes to the molecular orbitals of the corresponding maximum H_2-adsorbed complex. The results presented in Fig. 4 demonstrate that the electron density of M atoms increases in the following order: Ca > Ti ≃ Sc > Li ≃ V > Be. This finding suggests that the Ca atom adsorbs more H_2 molecules than the other atoms. Furthermore, in all of the complexes, the orbital electron density is predominantly distributed around -2 eV, situated in the low-energy region below the Fermi level for the respective atoms. Consequently, the capability of H_2 adsorption on the NH_2Ca^+ compound is greater, leading to the following hierarchy of H_2 adsorption ability: $NH_2Ca^+ > NH_2Sc^+ \simeq NH_2Ti^+ > NH_2Li^+ \simeq NH_2V^+ > NH_2Be^+$.

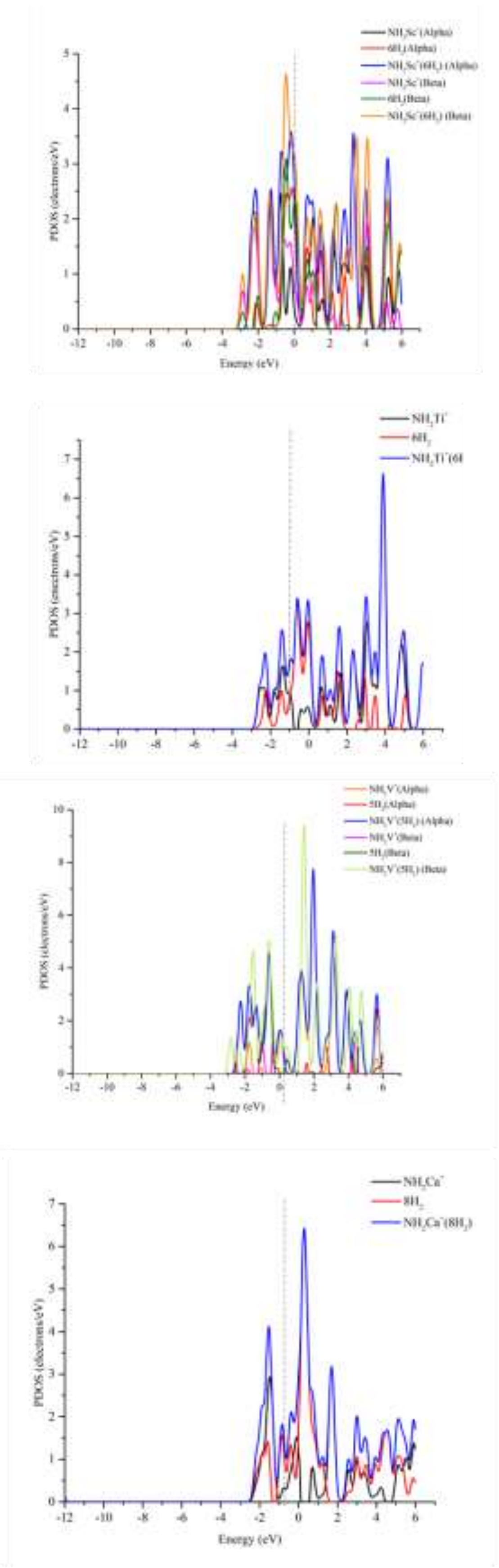

Fig. 4. Partial density of state (PDOS) plot for NH2M+(nH2) complex, where M is Be, Li, Sc, Ti, V, and Ca.

The bond lengths of NH_2M^+ compounds, both prior to and following H2 adsorption, have been calculated and are presented in Table 2. The N-H bond lengths remained unchanged across all considered complexes following H_2 adsorption. In the NH_2V^+ compound, the N-V bond length decreases by 0.3 Å after H_2 molecule adsorption, while the N-M bond lengths (where M = Be, Li, Sc, Ti, V, and Ca) in the other complexes increase, indicating a strengthening of the M-H_2 bond. The average distances between the adsorbed H_2 molecules and the M atom in the NH_2M^+ complexes range from 1.76 to 2.80 Å, suggesting that H_2 molecules can be adsorbed rapidly in these complexes. The H-H bond lengths remain nearly consistent across all studied complexes. Notably, the interaction between the adsorbed H_2 molecules and the M atom exhibits Kubas interaction, as evidenced by the elongation of the H-H bond compared to that of an isolated H_2 molecule. Previous research by Ahmad et al. [52] has also identified Kubas interaction between adsorbed H_2 molecules and sc-metallacarborane.

Table 2. Different bond lengths (Å) in $NH_2M^+(nH_2)$ complexes at MP2/6-311++g(d,p) level (The values in the parenthesis are corresponding values of bond lengths before H_2 molecules adsorption) where M is Be, Li, Sc, Ti, V, and Ca.

System		N-H	N-M	M-H_2	H-H
$NH_2M^+(nH_2)$	$NH_2Be^+(3H_2)$	1.01 (1.01)	1.49 (1.46)	1.76	0.76
	$NH_2Li^+(5H_2)$	1.02 (1.02)	2.04 (2.01)	2.24	0.74
	$NH_2Sc^+(6H_2)$	1.02 (1.02)	2.01 (1.98)	2.27	0.76
	$NH_2Ti^+(6H_2)$	1.02 (1.02)	1.92 (1.84)	2.03	0.77
	$NH_2V^+(5H_2)$	1.02 (1.02)	1.79 (2.09)	1.90	0.80
	$NH_2Ca^+(8H_2)$	1.02 (1.02)	2.22 (2.20)	2.80	0.74

The comparison of bond lengths in H_2-adsorbed NH_2M^+ complexes indicates that the adsorption strength of the H_2 molecule on these complexes follows the trend: $NH_2Be^+ > NH_2V^+ > NH_2Ti^+ > NH_2Li^+ > NH_2Sc^+ > NH_2Ca^+$.

Table 3. Calculations averaged adsorption energy without (ΔE), and with zero point energy correction (ΔE_{ZPE}), Gibbs free energy corrected adsorption energies (ΔE_G) in eV at 298.15 K and storage gravimetric density (%W) of $NH_2M^+(nH_2)$ where M is Be, Li, Sc, Ti, V, and Ca at wB97XD/6-311++G(d, p) level. (The values in parenthesis is at MP2/6-311++G (d, p) level).

System		Energy (eV)			W%
		ΔE	ΔE_{ZPE}	ΔE_G	
$NH_2M^+(nH_2)$	$NH_2Be^+(3H_2)$	0.64 (0.64)	0.48 (0.47)	0.20 (0.20)	19.3
	$NH_2Li^+(5H_2)$	0.17 (0.13)	0.07 (0.05)	-0.18 (-0.18)	30.3
	$NH_2Sc^+(6H_2)$	0.31 (0.18)	0.18 (0.07)	-0.08 (-0.19)	16.4
	$NH_2Ti^+(6H_2)$	0.43 (0.50)	0.26 (0.33)	-0.03 (0.05)	15.8
	$NH_2V^+(5H_2)$	0.58 (0.66)	0.39 (0.46)	0.10 (0.16)	12.9
	$NH_2Ca^+(8H_2)$	0.16 (0.12)	0.06 (0.04)	-0.19 (-0.19)	22.2

In the next phase of the study, the average hydrogen adsorption energies without zero-point energy correction (ΔE), with zero-point energy correction (ΔE_{ZPE}), and with Gibbs free energy correction (ΔE_G) were calculated at 298.15 K and 1 atm pressure for the specified complexes. The results are summarized in Table 3. The values of ΔE and ΔE_{ZPE} are positive for all complexes at both computational levels. These positive values at the MP2 and DFT computational levels follow the trend outlined below:

$NH_2Be^+(3H_2)$ > $NH_2V^+(5H_2)$ > $NH_2Ti^+(6H_2)$ > $NH_2Sc^+(6H_2)$ > $NH_2Li^+(5H_2)$ > $NH_2Ca^+(8H_2)$

This conclusion is drawn from Table 3, which indicates that the $NH_2Be^+(3H_2)$ and $NH_2V^+(5H_2)$ complexes exhibit positive Gibbs free energy corrected adsorption energies (ΔE_G) at both computational levels. This demonstrates that the formation of these complexes is thermodynamically favorable under ambient conditions. At the MP2/6-31++G (d, P) level, the $NH_2Be^+(3H_2)$, $NH_2Ti^+(6H_2)$, and $NH_2V^+(5H_2)$ complexes have an ΔE_G of 0.2, 0.05, and 0.16 eV, indicating that H_2 adsorption on these complexes is feasible at room temperature and occurs spontaneously. However, other complexes with slightly negative ΔE_G values are unable to adsorb H_2 molecules at room temperature.

In this study, we examined the gravimetric density of H_2 storage using the following equations:

$$H_2\ (\%W) = \left[\frac{M_{H2}}{M_{H2} + M_{host}}\right] \times 100 \tag{6}$$

In this context, M_{H2} and M_{host} represent the mass of the total number of adsorbed H_2 molecules and the NH_2M^+ compounds, respectively. The NH_2Be^+, NH_2Li^+, NH_2Sc^+, NH_2Ti^+, NH_2V^+, and NH_2Ca^+ compounds exhibit gravimetric hydrogen uptake capacities of 19.3, 30.3, 16.4, 15.8, 12.9, and 22.2%, respectively, with the capability to interact with a maximum of three, five, six, six, five, and eight H_2 molecules, respectively. As demonstrated in Table 3, the hydrogen uptake capacities of all studied complexes exceed the target established by the U.S. Department of Energy, which is set at 5.5 Wt% by 2025. A comparative analysis confirms that all desired complexes possess higher H_2 uptake capacities than previously reported compounds for hydrogen storage. Notably, this study marks the first instance of NH_2Be^+ compounds being able to adsorb three H_2 molecules.

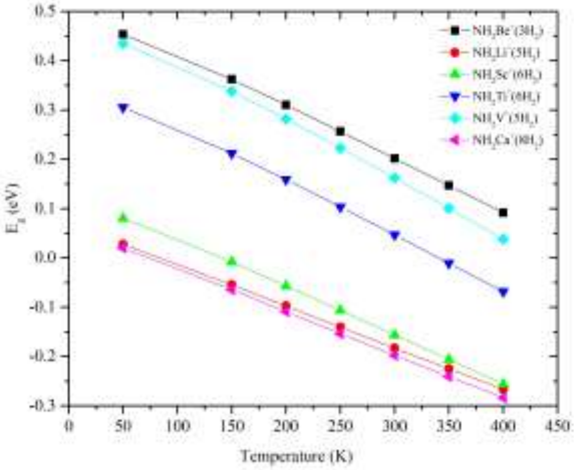

Fig. 5. (Color online) temperature dependent Gibbs free energy corrected H2 adsorption energies for NH2M+(nH2) complex, where M is Be, Li, Sc, Ti, V, and Ca (MP2/6-311++G(d,p) level).

The next step involves examining the effects of varying temperatures and pressures on H_2 adsorption, utilizing Gibbs free energy corrected adsorption energy changes across a broad spectrum of temperatures (from 50 K to 400 K) and pressures (from 50 atm to 400 atm) as illustrated in Figures 5 and 6. The findings indicate that H_2 adsorption on NH_2Be^+ and NH_2V^+ compounds is thermodynamically feasible across the range of pressures and temperatures analyzed. Notably, the temperature and pressure-dependent ΔE_G values for these complexes are more positive compared to other complexes. Interestingly, for the other complexes, the Gibbs free energy corrected adsorption energies are positive at lower temperatures and negative at all pressures examined, except for the $NH_2Ti^+(6H_2)$ complex, for which H_2 molecule adsorption is favorable below 350 K across all pressures considered. Therefore, the NH_2Be^+, NH_2V^+, and NH_2Ti^+ compounds present promising materials for H_2 storage, as the Gibbs free energy corrected adsorption energies remain positive over a wide range of temperatures and pressures.

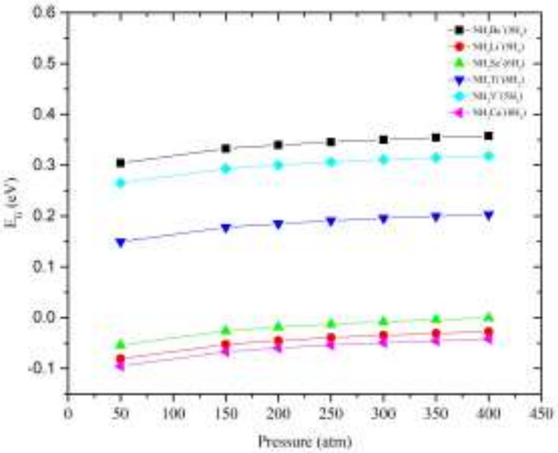

Fig. 6. (Color online) pressure dependent Gibbs free energy corrected H2 adsorption energies for NH2M+(nH2), where M is Be, Li, Sc, Ti, V, and Ca (MP2/6-311++G(d,p) level).

Another objective of this research is to assess the electrical response of these complexes by analyzing the gap between the highest occupied molecular orbitals (HOMO) and the lowest unoccupied molecular orbitals (LUMO), as illustrated in Fig. 7. The variation in the HOMO-LUMO gap (HLG) of the complexes before and after the adsorption of H_2 molecules has depicted in this figure. It is evident from Fig. 7 that the HLG of the NH_2Be^+ and NH_2V^+ compounds increases significantly following H_2 adsorption, while the $NH_2Li^+(6H_2)$ complex remains unchanged and exhibits the highest HLG energy. In other complexes, the HLG increases moderately after H_2 adsorption. The HLG for the NH_2M^+ complexes with maximum H_2 adsorption ranges from 10.0 to 15.8 eV. Ultimately, it can be concluded that the NH_2Be^+ and NH_2V^+ compounds within the NH_2M^+ series exhibit the highest electrical response, characterized by the largest change in HLG.

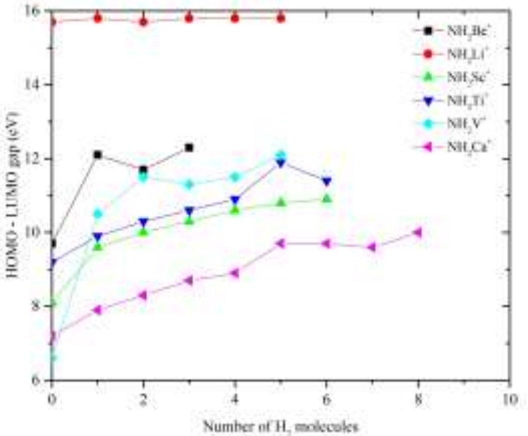

Fig. 7. (Color online) energy gap between highest occupied and lowest unoccupied molecular orbital for NH2M+(nH2), where M is Be, Li, Sc, Ti, V, and Ca (MP2/6-311++G(d, p) level).

The next step involves measuring the H_2 desorption temperatures from NH_2M^+ complexes using the van't Hoff equation (see Table 4). The H_2 desorption temperatures for the NH_2Be^+, NH_2Li^+, NH_2Sc^+, NH_2Ti^+, NH_2V^+, and NH_2Ca^+ complexes at the DFT (MP2) computational level are 617 (604), 90 (64), 238 (86), 329 (420), 506 (587), and 77 (51) K, respectively. Desorption temperatures increase in the following order: $NH_2Be^+ > NH_2V^+ > NH_2Ti^+ > NH_2Sc^+ > NH_2Li^+ > NH_2Ca^+$. The results indicate that H_2 desorption from the NH_2Be^+, NH_2V^+, and NH_2Ti^+ complexes is stronger than from the other complexes, which aligns with findings from other analyses. Notably, the $NH_2Be^+(3H_2)$ complex exhibits the highest H_2 desorption temperature, while the $NH_2Ca^+(8H_2)$ complex shows the lowest temperature among the $NH_2M^+(nH_2)$ complexes. This observation suggests that the interaction with adsorbed H_2 molecules is stronger at higher desorption temperatures. Additionally, the desorption temperatures of the NH_2Sc^+ and NH_2Ti^+ complexes are 238 and 329 K at the wB97XD/6-31++G (d, p) level, indicating thermodynamic favorability under ambient conditions.

Fig. 8 shows the trajectories of H_2 molecules from the metal atom during ADMP-MD simulations. The ADMP simulations start with an optimized structure at wB97XD/6-31++G (d, p) level as the initial geometry for the simulation. As can be seen from Fig. 8, all the adsorbed H_2 molecules in the initial structure do not remain adsorbed on NH_2M^+ complexes. Some of the H_2 molecules fly away from the complex during the simulation. Two, two, three, four, three, two H_2 molecules remain adsorbed on NH_2Be^+, NH_2Li^+, NH_2Sc^+, NH_2Ti^+, NH_2V^+, and NH_2Ca^+ compounds during the ADMP-MD simulations.

Table 4. Desorption temperature (TD) in Kelvin for NH2M+(nH2) where M is Be, Li, Sc, Ti, V, and Ca complexes utilizing the wB97XD and MP2 methods with 6-31++G(d, p) basis set.

System		wB97XD	MP2
$NH_2M^+(nH_2)$	$NH_2Be^+(3H_2)$	617	604
	$NH_2Li^+(5H_2)$	90	64
	$NH_2Sc^+(6H_2)$	238	86
	$NH_2Ti^+(6H_2)$	329	420
	$NH_2V^+(5H_2)$	506	587
	$NH_2Ca^+(8H_2)$	77	51

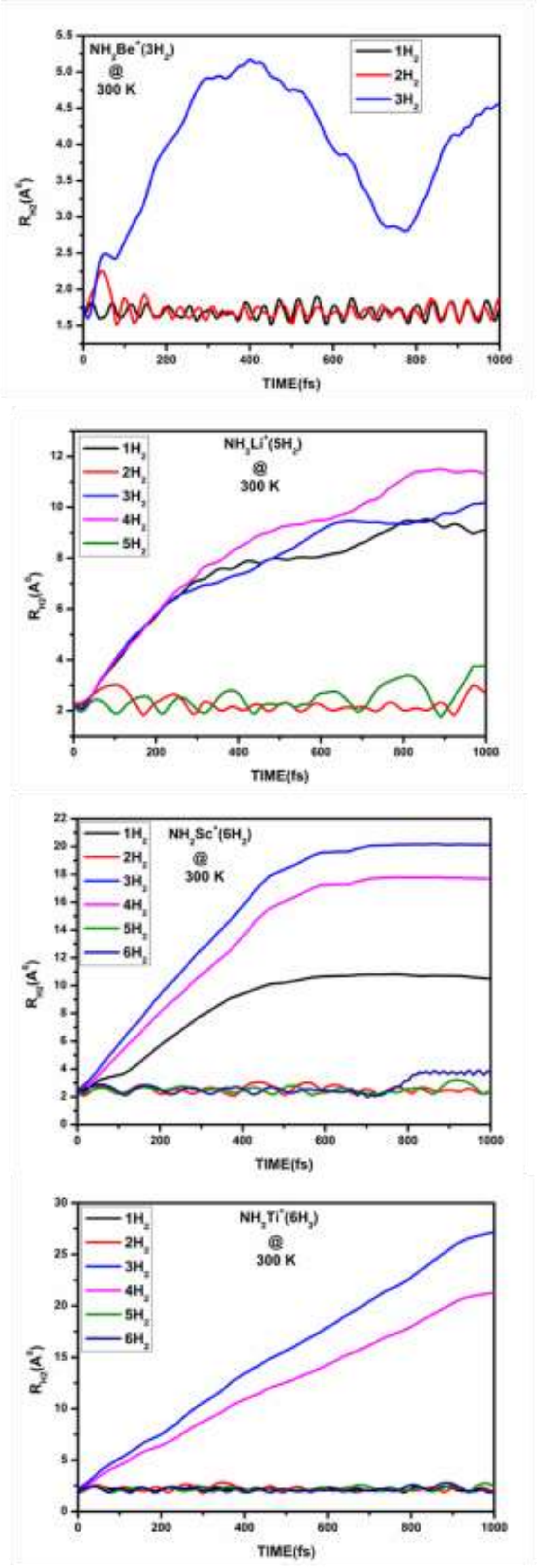

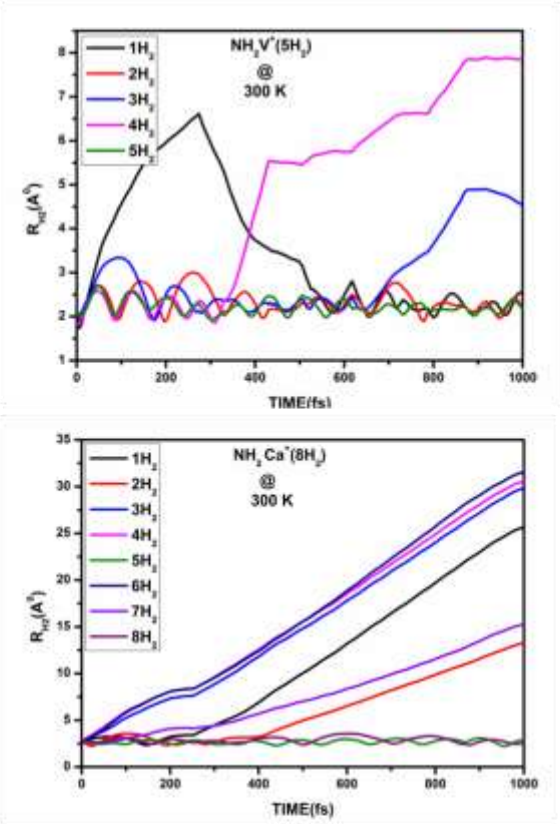

Fig. 8. Trajectories of the time evolution of distance of H2 molecules from M in the NH2M+ (nH2) complexes at 300 K. Where the M is Be, Li, Sc, Ti, V, and Ca.

We will now summarize the results of this study: According to PDOS analysis, the NH_2Ca^+ compound exhibits a greater capacity for H_2 molecule adsorption compared to other complexes, attributed to the higher electron density on the Ca atom. The NH_2Be^+, NH_2Li^+, NH_2Sc^+, NH_2Ti^+, NH_2V^+, and NH_2Ca^+ compounds can interact with a maximum of three, five, six, six, five, and eight H_2 molecules, respectively, thereby demonstrating a higher H_2 uptake capacity than previously reported compounds for hydrogen storage. The gravimetric density of hydrogen storage (%W) for all considered complexes exceeds the target established by the US Department of Energy (5.5 wt% by 2025). The NH_2Ti^+ compound has been identified as more suitable material for hydrogen storage because:

1. The H_2 molecule demonstrates optimal adsorption characteristics owing to its minimal M-H_2 bond lengths, with desorption temperatures ranging 329 K, making it suitable for vehicular applications under ambient conditions.
2. The positive values of ΔE, ΔE_{ZPE}, and ΔE_G at the MP2 and DFT computational levels indicate that the formation of these complexes is thermodynamically favorable under ambient conditions.
3. The corrected Gibbs free energy of adsorption remains positive over a wide range of temperatures and pressures.
4. The hydrogen uptake capacities of all studied complexes exceed the target established by the U.S. Department of Energy.

4. Conclusions

This study utilized density functional theory (DFT) and second-order Møller-Plesset perturbation theory (MP2) to assess the hydrogen storage capabilities of NH2M+ compounds (M = Be, Li, Sc, Ti, V, Ca). The results reveal that NH2Be+, NH2Li+, NH2Sc+, NH2Ti+, NH2V+, and NH2Ca+ complexes can bind up to three, five, six, six, five, and eight H2 molecules, respectively, with gravimetric hydrogen uptake capacities of 19.3%, 30.3%, 16.4%, 15.8%, 12.9%, and 22.2%. These capacities significantly exceed the U.S. Department of Energy’s 2025 target of 5.5 wt%. However, atom-centered density matrix propagation molecular dynamics (ADMP-MD) simulations indicate lower H2 uptake compared to DFT and MP2 results. Notably, NH2Be+, NH2Ti+, and NH2V+ complexes demonstrate thermodynamically favorable H2 adsorption across a wide range of temperatures (50–400 K) and pressures (50–400 atm), with positive Gibbs free energy-corrected adsorption energies, indicating spontaneous adsorption at ambient conditions. These complexes also exhibit the highest H2 desorption temperatures, reflecting strong interactions with H2 molecules. Additionally, NH2Be+ and NH2V+ show the most significant changes in HOMO-LUMO gap (HLG), indicating a robust electrical response. Among the studied compounds, NH2Ti+ stands out as a highly promising candidate for hydrogen storage under ambient conditions due to its exceptional adsorption characteristics and high capacity.

Conflict of interests

The authors report no declarations of interest.

Data Availability Statement

Data sets generated during the current study are available from the corresponding author (M. Solimannejad) on reasonable request.

Acknowledgements

The authors gratefully acknowledge the financial support of the University of Qom.

Author contributions

Rezvan Rahimi: Software, Investigation, Writing – original draft.

Mohammad Solimannejad: Conceptualization, Validation, Reviewing, and Editing.
Ajay Chaudhari: Validation, Reviewing, and Editing.

References

[1] Crabtree GW, Dresselhaus MS, Buchanan M V. The Hydrogen Economy. Physics Today 2004;57:39–44. https://doi.org/10.1063/1.1878333.

[2] Jain IP. Hydrogen the fuel for 21st century. International Journal of Hydrogen Energy 2009;34:7368–78. https://doi.org/10.1016/j.ijhydene.2009.05.093.

[3] Berry GD, Pasternak AD, Rambach GD, Ray Smith J, Schock RN. Hydrogen as a future transportation fuel. Energy 1996;21:289–303. https://doi.org/10.1016/0360-5442(95)00104-2.

[4] Principi G, Agresti F, Maddalena A, Lo Russo S. The problem of solid state hydrogen storage. Energy 2009;34:2087–91. https://doi.org/10.1016/j.energy.2008.08.027.

[5] https://energy.gov/eere/fuelcells/doe-technical-targetsonboard-hydrogen-storage-light-duty-vehicles.

[6] Schüth F. Hydrogen and hydrates. Nature 2005;434:712–3. https://doi.org/10.1038/434712a.

[7] Shin-ichi Orimo , Yuko Nakamori , Jennifer R. Eliseo , Andreas Züttel and, Craig M. Jensen. Complex Hydrides for Hydrogen Storage 2007. https://doi.org/10.1021/cr0501846.

[8] Liu J, Yu J, Ge Q. Hydride-Assisted Hydrogenation of Ti-Doped NaH/Al: A Density Functional Theory Study. The Journal of Physical Chemistry C 2011;115:2522–8. https://doi.org/10.1021/jp108651s.

[9] T. J. Dhilip Kumar *, Philippe F. Weck and, Balakrishnan N. Evolution of Small Ti Clusters and the Dissociative Chemisorption of H2 on Ti 2007. https://doi.org/10.1021/jp068782r.

[10] Tarakeshwar P, Kumar TJD, Balakrishnan N. Hydrogen multicenter bonds and reversible hydrogen storage. The Journal of Chemical Physics 2009;130:114301. https://doi.org/10.1063/1.3082130.

[11] McKeown NB, Gahnem B, Msayib KJ, Budd PM, Tattershall CE, Mahmood K, et al. Towards Polymer-Based Hydrogen Storage Materials: Engineering Ultramicroporous Cavities within Polymers of Intrinsic Microporosity. Angewandte Chemie International Edition 2006;45:1804–7. Microporous Polymers. https://doi.org/10.1002/anie.200504241.

[12] Ma L-J, Jia J, Wu H-S, Ren Y. Ti–η2-(C2H2) and HCC–TiH as high capacity hydrogen storage media. International Journal of Hydrogen Energy 2013;38:16185–92. https://doi.org/10.1016/j.ijhydene.2013.09.151.

[13] Ma L-J, Jia J, Wu H-S. Computational investigation of hydrogen storage on scandium–acetylene system. International Journal of Hydrogen Energy 2015;40:420–8. https://doi.org/10.1016/j.ijhydene.2014.10.136.

[14] Kalamse V, Wadnerkar N, Deshmukh A, Chaudhari A. C2H2M (M = Ti, Li) complex: A possible hydrogen storage material. International Journal of Hydrogen Energy 2012;37:3727–32. https://doi.org/10.1016/j.ijhydene.2011.05.061.

[15] Tavhare P, Kalamse V, Bhosale R, Chaudhari A. Interaction of molecular hydrogen with alkali and transition metal-doped acetylene complexes. Structural Chemistry 2015;26:823–9. https://doi.org/10.1007/s11224-014-0547-7.

[16] Bandaru S, English NJ, Phillips AD, MacElroy JMD. Towards the design of novel boron- and nitrogen-substituted ammonia-borane and bifunctional arene ruthenium catalysts for hydrogen storage. Journal of Computational Chemistry 2014;35:891–903. https://doi.org/10.1002/jcc.23534.

[17] Samolia M, Kumar TJD. A conceptual DFT study of the hydrogen trapping efficiency in metal functionalized BN system. RSC Adv 2014;4:30758–67. https://doi.org/10.1039/C4RA03707C.

[18] Konda R, Kalamse V, Deshmukh A, Chaudhari A. Closoborate-transition metal complexes for hydrogen storage. RSC Advances 2015;5:99207–16. https://doi.org/10.1039/C5RA12927C.

[19] Lu QL, Meng JW, Song WJ, Wan JG. High capacity hydrogen storage in closo-hexaborate dianion B6H62−. International Journal of Hydrogen Energy 2013;38:13328–34. https://doi.org/10.1016/j.ijhydene.2013.07.085.

[20] Tavhare P. Boron substitution effect on adsorption of H2 molecules on organometallic complexes. International Journal of Hydrogen Energy 2019;44:345–53. https://doi.org/10.1016/j.ijhydene.2018.02.118.

[21] Konda R, Deshmukh A. Alkali, alkaline earth and transition metal doped B6H6 complexes for hydrogen storage. International Journal of Hydrogen Energy 2017;42:23723–30. https://doi.org/10.1016/j.ijhydene.2017.05.023.

[22] Kalamse V, Krishna R. Boron substituted and un-substituted aromatic complexes as hydrogen storage media. International Journal of Hydrogen Energy 2016;41:11723–9. https://doi.org/10.1016/j.ijhydene.2015.11.171.

[23] Kalamse V, Tavhare P, Deshmukh A, Krishna R. Effect of boron substitution on hydrogen storage capacity of Li and Ti decorated naphthalene. International Journal of Hydrogen Energy 2017;42:23716–22. https://doi.org/10.1016/j.ijhydene.2017.02.107.

[24] Deshmukh A, Konda R, Titus E, Chaudhari A. Electronic structure calculations and molecular dynamics simulations of hydrogen adsorption on Beryllium doped complexes. International Journal of Hydrogen Energy 2017;42:23708-15. https://doi.org/10.1016/j.ijhydene.2017.02.118.

[25] Tavhare P, Wadnerkar N, Kalamse V, Chaudhari A. H 2 Interaction with C 2 H 2 TM (TM= Sc, Ti, V) Complex Using Quantum Chemical Methods. Acta Physica Polonica, A 2016;129:6. https://doi.org/10.12693/APhysPolA.129.1257.

[26] Deshmukh A, Chiu CC, Chen YW, Kuo JL. Tunable gravimetric and volumetric hydrogen storage capacities in polyhedral oligomeric silsesquioxane frameworks. ACS applied materials & interfaces 2016; 8:25219-28. https://doi.org/10.1021/acsami.6b06245.

[27] Deshmukh A, Konda R, Kalamse V, Chaudhari A. Improved H 2 uptake capacity of transition metal doped benzene by boron substitution. RSC Advances 2016; 6:47033-42. https://doi.org/10.1039/C6RA06483C.

[28] Wadnerkar N, Kalamse V, Chaudhari A. Hydrogen uptake capacity of C2H4Sc and its ions: a density functional study. Journal of computational chemistry 2010; 31:1656-61. https://doi.org/10.1002/jcc.21449.

[29] Kalamse V, Wadnerkar N, Chaudhari A. Hydrogen storage in C2H4V and C2H4V+ organometallic compounds. The Journal of Physical Chemistry C 2010; 114:4704-9. https://doi.org/10.1021/jp910614n.

[30] Wadnerkar N, Kalamse V, Chaudhari A. Higher hydrogen uptake capacity of C 2 H 4 Ti+ than C 2 H 4 Ti: a quantum chemical study. Theoretical Chemistry Accounts 2010; 127:285-92. https://doi.org/10.1007/s00214-009-0714-x.

[31] Pathak B, Pradhan K, Hussain T, Ahuja R, Jena P. Functionalized boranes for hydrogen storage. ChemPhysChem 2012; 13:300-4. https://doi.org/10.1002/cphc.201100585.

[32] Bergstrom FW, Fernelius WC. The Chemistry of the Alkali Amides. Chemical Reviews 1933; 12:43-179. https://doi.org/10.1021/cr60041a002.

[33] Juza R. Amides of the alkali and the alkaline earth metals. Angewandte Chemie International Edition in English 1964; 3:471-81. https://doi.org/10.1002/anie.196404711.

[34] Power PP, Sanger AR, Srivastava RC. Metal and Metalloid Amides. Ellis Harwood: Chichester, England. 1980:0020-1669. https://doi.org/10.1021/ed058pA315.2.

[35] Bram G, Bataille X. Albin Haller et l'amidure de sodium: la naissance de la chimie des bases fortes. Comptes Rendus de l'Académie des Sciences-Series IIB-Mechanics-Physics-Chemistry-Astronomy 1997; 324:653-7. https://doi.org/10.1016/S1251-8069(97)83184-3.

[36] Freeman R, Richards RE. The proton magnetic resonance spectrum of potassium amide. Transactions of the Faraday Society 1956; 52:802-6. https://doi.org/10.1039/TF9565200802.

[37] Mason SF. The Structure of the Amide Ion. The Journal of Physical Chemistry 1957; 61:384. https://doi.org/10.1021/j150549a035.

[38] Minella CB, Rongeat C, Domènech-Ferrer R, Lindemann I, Dunsch L, Sorbie N, Gregory DH, Gutfleisch O. Synthesis of LiNH 2+ LiH by reactive milling of Li 3 N. Faraday discussions.2011;151:253-62. https://doi.org/10.1039/C1FD00009H.

[39] Sun Q, Qin M, Bu Y, Han K. Structural properties and electron transfer reactivity of NX3/NX3+ (X= H, F) coupling systems. Journal of Molecular Structure: THEOCHEM 2005; 714:165-74. https://doi.org/10.1016/j.theochem.2004.09.043.

[40] Huntress Jr WT, Mosesman MM, Elleman DD. Relative Rates and Their Dependence on Kinetic Energy for Ion–Molecule Reactions in Ammonia. The Journal of Chemical Physics 1971; 54:843-9. https://doi.org/10.1063/1.1675008.

[41] Huntress Jr WT, Pinizzotto Jr RF. Product distributions and rate constants for ion-molecule reactions in water, hydrogen sulfide, ammonia, and methane. The Journal of Chemical Physics 1973; 59:4742-56. https://doi.org/10.1063/1.1680687.

[42] Tomoda S, Suzuki S, Koyano I. State selected ion–molecule reactions by a coincidence technique. XV. Hydrogen atom abstraction as an electron jump followed by proton transfer in the ND+ 3 (v)+ NH3 and NH+ 3 (v)+ ND3 reactions. The Journal of chemical physics 1988; 89:7268-76. https://doi.org/10.1063/1.455307.

[43] Tachikawa H, Tomoda S. A theoretical study on the vibrationally state-selected hydrogen transfer reaction: NH+ 3 (v)+ NH3→ NH+ 4+ NH2. An ab initio MR-SD-CI and classical trajectory approach. Chemical physics 1994; 182:185-94. https://doi.org/10.1016/0301-0104(94)00040-9.

[44] Sun Q, Bu Y, Sun L, Yan S, Cheng X. Electron transfer reactivity of methyl-substituted amine NHn (CH3) 3− n/NHn (CH3)(n= 0–3) self-exchange systems: a theoretical investigation. Journal of physical organic chemistry 2005; 18:69-82. https://doi.org/10.1002/poc.802.

[45] Møller C, Plesset MS. Note on an approximation treatment for many-electron systems. Physical review 1934; 46:618. https://doi.org/10.1103/PhysRev.46.618.

[46] Frisch MJ, Pople JA, Binkley JS. Self-consistent molecular orbital methods 25. Supplementary functions for Gaussian basis sets. The Journal of chemical physics 1984; 80:3265-9. https://doi.org/10.1063/1.447079.

[47] Frisch MJ, Trucks GW, Schlegel HB, Scuseria GE, Robb MA, Cheeseman JR, Scalmani G, Barone V, Mennucci B, Petersson G, Nakatsuji H. Gaussian 09, revision a. 02, gaussian. Inc., Wallingford, CT 2009;200:28.

[48] O'boyle NM, Tenderholt AL, Langner KM. Cclib: a library for package-independent computational chemistry algorithms. Journal of computational chemistry 2008; 29:839-45. https://doi.org/10.1002/jcc.20823.

[49] Reed AE, Weinstock RB, Weinhold F. Natural population analysis. The Journal of Chemical Physics 1985; 83:735-46. https://doi.org/10.1063/1.449486.

[50] Tavhare P, Titus E, Chaudhari A. Boron substitution effect on adsorption of H2 molecules on organometallic complexes. International Journal of Hydrogen Energy 2019; 44:345-53. https://doi.org/10.1016/j.ijhydene.2018.02.118.

[51] Lide DR. CRC handbook of chemistry and physics: a ready-reference book of chemical and physical data. CRC press 1995.

[52] Ahmad R, Bora PL, Singh AK. “Capping” out oxygen interference: An approach to achieve efficient hydrogen storage via Kubas binding. International Journal of Hydrogen Energy 2016; 41:5979-85. https://doi.org/10.1016/j.ijhydene.2016.02.081.